Ecological Modelling 484 (2023) 110487

Contents lists available at ScienceDirect

Ecological Modelling

journal homepage: www.elsevier.com/locate/ecolmodel

Sector aggregation effect on embodied carbon emission based on city-centric global multi-region input-output (CCG-MRIO) model

Duo Xu [a], Gengyuan Liu [a,b,*], Fanxin Meng [a], Ningyu Yan [c,d], Hui Li [a], Feni Agostinho [a,e], Cecilia MVB Almeida [a,e], Biagio F Giannetti [a,e]

[a] State Key Joint Laboratory of Environment Simulation and Pollution Control, School of Environment, Beijing Normal University, Beijing, 100875, China
[b] Beijing Engineering Research Center for Watershed Environmental Restoration & Integrated Ecological Regulation, Beijing, 100875, China
[c] Key Laboratory for City Cluster Environmental Safety and Green Development of the Ministry of Education, Institute of Environmental and Ecological Engineering, Guangdong University of Technology, Guangzhou, 510006, China
[d] Southern Marine Science and Engineering Guangdong Laboratory (Guangzhou), Guangzhou, 511458, China
[e] Post-graduation Program in Production Engineering, Paulista University, Brazil

ARTICLE INFO

Keywords:
City-centric global multi-region input-output model
Sector aggregation effect
Embodied carbon emission
Structural decomposition analysis
Structural path analysis

ABSTRACT

Sector aggregation under the input-output framework may lead to deviation in results and the lack of detailed sectoral information, which hinder the targeted implementation of accurate sectoral adjustment policies. This paper explores the effects of sector aggregation on the embodied carbon emission of the residential consumptions of Beijing and Shanghai based on the city-centric global multi-region input-output (CCG-MRIO) model. Integrating with structural path analysis and structural decomposition analysis, the impacts of sector aggregation on the identifying of critical emission transmission paths and driving forces are also revealed. Three sector aggregation datasets are discussed to track the sector aggregation effect in 2012 and 2017. The findings show that the carbon emission results at 8 sector level better align with the results at the 22 sector level than those at 32 sector level. Moreover, sector aggregation will lead to the absence of some critical carbon transmission paths, some factor contributions on carbon emission also changed their directions at different sector levels. On the basis of clarifying the sector aggregation effect on embodied carbon emission, the research results provide a reference for similar studies to select the appropriate level of sector aggregation, to realize the goal of simplifying the calculation or gaining more detailed sectoral emission information.

1. Introduction

With the globalization of trade, regional carbon emission especially the carbon emission embodied in inter-regional trade, have attracted the extensive attention of climate economists. With large population and active foreign trade, cities' growing residential consumptions have caused a large amount of embodied carbon emission along the supply chains among regions, which has become the main driver of carbon emission growth (Wang and Feng, 2021). Adopting sectoral carbon inventory as the satellite account, the multi-region input-output (MRIO) method has been widely used to study interregional linkages and their contribution to carbon emission (Zhou et al., 2018). Compared with the single-region input-output (SRIO) method, the MRIO table can describe input-output relationships between regions, which has important practical and research value for formulating emission reduction measures effectively through analysis of interregional trade flows.

The traditional MRIO model is based on the input-output table which contains several regions at an equal level, so only the inter-regional input-output relationship at the same regional level, such as between cities (Wang et al., 2020), or between countries (Dawkins et al., 2019), can be analyzed. It would be more scientific to integrate domestic trade and international trade into the same framework for comprehensive research, so the sources of embodied carbon emission from a city's residential consumption can be more comprehensively reflected, the city-centric global multi-region input-output (CCG-MRIO) model proposed by Lin et al. (2017) can realize such research need. However, building a CCG-MRIO model means higher data processing requirements, which will cause larger uncertainty in the sector integration process to make the sector classification of different databases consistent. Unfortunately, researchers often split or merge the sectors based on

* Corresponding author.
E-mail address: liugengyuan@bnu.edu.cn (G. Liu).

https://doi.org/10.1016/j.ecolmodel.2023.110487
Received 8 April 2023; Received in revised form 10 August 2023; Accepted 10 August 2023
Available online 14 August 2023

the national or international sector classification catalogs, the number of sectors after consolidation is random and the most detailed sectoral level available is not given priority, so the possible effect of different sector aggregation levels on embodied carbon emission results is usually ignored. Such neglect may lead to the loss of available information if the sectoral disaggregation can bring accurate and additional information, or unnecessary complex data processing if the goal is only to locate some highly aggregated sectors with significant emission contributions or focus on regional emission contributions. Although some scholars have tried to analyze the sectoral aggregation effect on the analysis results in single-region studies (Su et al., 2010) and multi-region analysis (Bouwmeester and Oosterhaven, 2013; de Koning et al., 2015; Zhang et al., 2019), there is still a lack of sectoral aggregation research on the CCG-MRIO analysis, especially for the detailed discussion on the effect of sector aggregation on embodied carbon emission flows and the contribution of emission drivers. For the CCG-MRIO tables that need to be constructed by researchers themselves, the impact of sectoral aggregation on carbon emission based on this table may be more obvious than that of traditional MRIO table.

This study aims to reveal how sector aggregation affects the embodied carbon emission changes in CCG-MRIO results. Taking residential consumptions of Beijing and Shanghai with international trade activities as examples, the sectoral and regional contribution results, factor contribution results based on structural decomposition analysis (SDA) and critical path results based on structural path analysis (SPA) are studied. The contribution of this paper is to give a detailed analysis of the sectoral aggregation effect on regional consumption-side embodied carbon emission, and the empirical research results show the trade-off between using assumptions to make up for data defects and not using assumptions to give up additional sector information, and provide possible scenarios for highly aggregated sector level that can simplify calculations.

2. Literature review

As a research tool for interregional trade linkages in goods and services, the MRIO method has been widely used to track the embodied carbon emission of final consumption (Liu et al., 2015). Residential consumption is an important component of regional carbon emission with the improvement of residential living standards (Wang et al., 2019a), so examining the source and change of the carbon emission embodied in residential consumption is significant for regional carbon emission control. Scholars have studied the embodied carbon emission of residential consumption at various spatial scales based on the MRIO method. Ma et al. (2022) used the MRIO method and consumption expenditure data to study the regional carbon emission of residential consumption in China, and they found that the carbon emission in the southeast region is the largest. Liu et al. (2022) adopted the MRIO method to investigate the regional disparity change trends of urban residential embodied carbon emission from 2002 to 2012 in China, they found that the eastern regions have larger emission growth and the western regions have faster emission increase rates. With the increasing development of international trade, some scholars began to put international trade into a single region's embodied carbon emission analysis, such as the embodied emission research of in China-India trade studied by Wang and Yang (2020), and the carbon flow research of China and its trading partners conducted by Yan et al. (2020). Under this background, Lin et al. (2017) have proposed the city-centric global multi-region input-output (CCG-MRIO) model to provide a bridge to analyze the relationship between individual cities and the utilization of sectoral products in various countries around the world to study further the city's consumption embodied carbon emission.

The contribution of each sector and region to the total embodied carbon emission can be obtained based on the MRIO analysis. Still, it tends to pursue more detailed research on the embodied emissions of input-output process between sectors and regions to reflect the changes more clearly in regional embodied carbon emission. The structural path analysis (SPA) has been used to identify the critical environmental transmission paths by tracing back the intricate production chains (Hong et al., 2016), the SPA uses the Tayler expansion equation of the Leontief inverse matrix to identify embodied carbon emission on each supply chains among sectors (Zhang et al., 2021). Growing literature uses it to find out the important embodied carbon emission transmission path among sectors. Fang and Yang (2021) used the structural path analysis method to identify the critical supply chain paths driving embodied carbon emission changes in Sichuan province. They found that the petroleum processing, agriculture, and transportation sectors are the key upstream sectors driving the growth of embodied carbon emission. Zhao et al. (2021) studied the carbon emission transmission path of China's electricity sector based on the structural path analysis method, and the results reflect that Eastern China and South China are the sources of inflow paths in consumption centers, while Central China, Guangdong and Jiangsu are the sources of outflow paths for production centers. Apart from the embodied carbon emission path, the SPA can also be applied to energy (Su et al., 2019; Yang et al., 2020), SO_2 emission (Wang et al., 2019b), energy-water nexus analysis (Shi et al., 2020; Wang and Chen, 2021) and other fields.

Many factors influence the embodied carbon emission changes, and the structural decomposition analysis (SDA) can study these factor contributions to embodied carbon emission changes at the sectoral and regional levels. Compare with another factor decomposition method as the index decomposition analysis (IDA) focus on the summary on emission changes, SDA is usually applied to study the demand-side effects and trade-related issues (Wang et al., 2017), and SDA can give a comprehensive analysis of direct and indirect effects (Hoekstra and van der Bergh, 2003; Su and Ang, 2012a). It has additional and multiplicative two decomposition forms. The additional form is used for the decomposition of absolute indicators, such as the total carbon emission (Cansino et al., 2016), while the multiplicative form is used for the decomposition of relative indicators, such as the carbon emission intensity (Su and Ang, 2017). In the carbon emission research adopting the SDA method, Xie et al. (2019) used the method to decompose the carbon emission changes of China's transportation industry into eight factors' contributions, including energy structure, energy intensity, input mix and five final use categories, they have found that the energy intensity factor played a dominant role in reducing emissions. Jiang et al. (2021) applied the method to decompose the global carbon emission change into six influencing factors as the carbon emission intensity, the domestic and international input structures, consumption pattern and consumption volume, and population, and the results have shown that the domestic input structure factor help to reduce largest carbon emission. Among various influencing factors, the carbon intensity factor, input-output structure factor and final demand factor are the three most common influencing factors that represent the impact of efficiency change, input-output structure change and demand change on the change of embodied carbon emission (Su and Ang, 2012b). Combined with the SPA method, a clear view of regional embodied carbon emission changes can be presented.

The sector aggregation effect is an issue that is easily often ignored but it is exist and is crucial in the environmental input-output research, the different choices of sector aggregation level lead to the discrepancy in embodied carbon emission results (Su et al., 2010). In dealing with such issue, Lenzen (2011) encourages the disaggregation of input-output data even based on few real data instead of the aggregation of environmental data. Steen-Olsen et al. (2014) suggest a high level of sectoral detail based on real data can significantly improve the accuracy of the results. Bouwmeester and Oosterhaven (2013) think that the specific aim of a study is a determining factor of the required sector level. de Koning et al. (2015) and Zhang et al. (2019) tend to use high resolution sector level and preserve as much sectoral detail as possible. The appropriate sector level is a comprehensive balance of research purpose, sector information details, computational complexity, and data accuracy, which may be more important in the CCG-MRIO model with complex data processing than traditional input-output models, and the comprehensive sector aggregation study on embodied carbon emission changes involve embodied emission flows and factor emission contributions in such model is still absent. Therefore, taking residential consumptions of Beijing and Shanghai with developed international trades as example, this paper examines how the sector aggregation level affects the embodied carbon emission results under the CCG-MRIO framework, so as to provide a reference for the subsequent research on the selection and treatment of sectoral aggregation level.

3. Method and data

3.1. Method

3.1.1. The embodied carbon emission based on the CCG-MRIO model

This paper introduces the adjustment proposed by Lin et al. (2017) to format a city-centric global multi-region input-output (CCG-MRIO) table, the detailed process and the schematic diagram are presented in **Appendix A**. The process to format the CCG-MRIO table is different from the embedded regional IO dataset into the global dataset proposed by Su et al. (2021), the latter focus on the disaggregation of China in the global WIOD dataset according to the interregional structure in China's MRIO dataset and regional bilateral trade with world countries in the global WIOD datasets, while the CCG-MRIO table formation committed to estimating the trade matrix between cities and their trade regions. The embodied carbon emission of local residential consumption is calculated as:

$$C_l = f^{'} L y_l = f_v^{'} H y_l = f^{'} H \sum y_{g,l} = \sum f_v^{'} H y_{g,l} \sum C_{g,l} \tag{1}$$

where the f is the carbon intensity vector of total output, f_v is the carbon intensity vector of value added, v is the integrated value added vector, $k = x/v$ is the primary input coefficient vector, L is the Leontief inverse matrix, $H = \hat{k}L$ is the value added requirement coefficient matrix, y_l is the vector of integrated local residential consumption, $y_{g,l}$ is the products input from region g to local residential consumption vector, $C_{g,l}$ is the embodied carbon emission vector of local residential consumption contributed by the products input from region g.

Based on the Eq. (1), the embodied carbon emission changes from base year 0 to research year 1 can be formulated as:

$$\begin{aligned}\Delta C_l &= \Delta C_l^1 - \Delta C_l^0 = f_v^{l,1'} H^1 y^1 - f_v^{l,0'} H^0 y^0 \\ &= \frac{1}{2}\left(f_v^{l,1'} - f_v^{l,0'}\right)\left(H^0 y^0 + H^1 y^1\right) \\ &+ \frac{1}{2} f_v^{l,0'}\left(H^1 - H^0\right) y^1 + \frac{1}{2} f_v^{l,1'}\left(H^1 - H^0\right) y^0 \\ &+ \frac{1}{2} f_v^{l,0'} H^0\left(y^1 - y^0\right) + \frac{1}{2} f_v^{l,1'} H^1\left(y^1 - y^0\right) \\ &= \Delta C_{ci}^l + \Delta C_{ps}^l + \Delta C_{fd}^l\end{aligned} \tag{2}$$

where the ci, ps, fd represent the carbon intensity factor (reflect the efficiency changes), input-output structure factor (reflect the input-output structure changes) and final demand factor (reflect the consumption demand changes), respectively. The ΔC_{ci}^l, ΔC_{ps}^l, and ΔC_{fd}^l represent contributions of carbon intensity factor, input-output factor, and final demand factor on local (Beijing and Shanghai) residential embodied carbon emission changes, respectively. The two-polar decomposition form proposed by Dietzenbacher and Los (1998) is used to obtain the contributions of these three factors to the embodied carbon emission changes in local residential consumption.

Based on the Talyor expansion of the Leontief inverse matrix (Wood and Lenzen, 2003), the structural path analysis is used to identify the transmission paths of embodied carbon emission among sectors of different regions as:

$$\begin{aligned}C_l &= f^{'} L y_l = f^{'}\left(I + A + A^2 + \ldots\right) y_l \\ &= \sum_{r=1}^{m}\sum_{i=1}^{n} f_i^r y_i^r + \sum_{r=1}^{m}\sum_{s=1}^{m}\sum_{i=1}^{n}\sum_{j=1}^{n} f_i^r A_{i,j}^{r,s} y_j^s + \sum_{r=1}^{m}\sum_{s=1}^{m}\sum_{t=1}^{m}\sum_{i=1}^{n}\sum_{j=1}^{n}\sum_{g=1}^{n} f_i^r A_{i,j}^{r,s} A_{j,g}^{s,t} y_g^t + \ldots\end{aligned} \tag{3}$$

where each addition item on the right side of the Eq. (3) represents a transmission path of embodied carbon emission, m is the total number of regions, n is the total number of sectors. r, s and t are the regional numbers, i,j and g are the sectoral numbers. A is the direct consumption coefficient matrix. To extract the key transmission path of embodied carbon emission effectively and reduce the computational complexity, the 0.1% threshold of the total embodied carbon emission is set to trim some trivial paths. Finally, 30 paths with the largest embodied carbon emission are identified to trace the sector aggregation effect on path results under three datasets.

3.1.2. Sector aggregation effect on embodied carbon emission

There are usually two sector levels in the environmental input-output studies, the first level is the sector classification level that retains the existing carbon emission data to the greatest extent, the second level is the sector classification level that retains the most detailed input-output sectoral data. We assume the first level has N sectors and the second level has M sectors, and N is usually lower than M. The relative change value proposed in Su et al. (2021) is used to quantify the sector aggregation effect (SAE) on the embodied carbon emission between the two sector aggregation levels as:

$$SAE = \frac{C_M - C_N}{C_N} \times 100\% \tag{4}$$

where the C_M is the embodied carbon emission at the M sector aggregation level, and the C_N is the embodied carbon emission at the N sector aggregation level. Similarly, based on the Eq. (4), the sector aggregation effect on the emission contributions of sectors can be formulated as:

$$SAE_g = \frac{C_{g,M} - C_{g,N}}{C_{g,N}} \times 100\% \tag{5}$$

where the SAE_g is the sector aggregation effect on the emission contribution of sector g. The sector aggregation effect on structural decomposition analysis results can be formulated as:

$$BSA_{ci} = \frac{\Delta C_{ci,M} - \Delta C_{ci,N}}{C_N^0} \times 100\% \tag{6}$$

$$BSA_{ps} = \frac{\Delta C_{ps,M} - \Delta C_{ps,N}}{C_N^0} \times 100\% \tag{7}$$

$$BSA_{fd} = \frac{\Delta C_{fd,M} - \Delta C_{fd,N}}{C_N^0} \times 100\% \tag{8}$$

where the BSA_{ci}, BSA_{ps}, and BSA_{fd} are the sector aggregation effects on the contributions of carbon intensity factor, input-output structure factor, and final demand factor, respectively. The sector aggregation effect on regional influencing factors' contributions to the embodied carbon emission can also be calculated on similar methods.

Different datasets contain three different sector levels in this paper. The first dataset is set as L1 dataset contains 8 sectors, it is a typical sector classification level for simplified calculation. The second dataset contains 22 sectors, it is the most detailed sector level by considering the available sectoral carbon emission data of all regions. The third dataset is set as L3 dataset contains 32 sectors, it is the most detailed sector level aggregated by considering the consistent sector classification data in different input-output tables, the consistent intensity assumption (it assume the carbon emission intensity of sub-sectors are consistent with that of their father sector) is applied to supplement the unavailable sectoral carbon emission data. The sectoral IDs, names, and corresponding relationships in three different datasets are given in **Appendix B**. It should be noted that the L2 dataset is defined as the basic dataset, for it ensures the most detailed sectoral classification on the available data, unlike L1 dataset with sector combination or L3 datasets with sector expansion. The results of L2 dataset are further aggregated into the 8-sector level of L1 dataset to make comparisons between L1 and L2 datasets, and the results of L3 dataset are further aggregated into the 22-sector level of L2 dataset to make comparisons between L2 and L3 datasets.

3.2. Data

Three kinds of input-output tables are involved in this paper, the inter-country input-output tables were obtained from the database of the Organization for Economic Co-operation and Development (OECD, 2021), the local input-output tables of Beijing and Shanghai were taken from the local statistics bureau, and the China provincial multi-region input-output tables were taken from the Carbon Emission Accounts and Datasets (CEADs, 2022). The sectoral carbon emission data from Shan et al. (2018) and Shan et al. (2020) were used for Beijing, Shanghai, and mainland China (the rest of mainland China by deducting Beijing and Shanghai, respectively), while the sectoral carbon emission data in carbon dioxide emissions embodied in international trade database from OECD were used for other regions. Local import and export trade data of Beijing and Shanghai are taken from their customs statistical database, while the import and export data of other regions/countries are taken from OECD database.

The residential carbon emission of Beijing and Shanghai from 2012 to 2017 are studied in this paper, while the 2017 input-output table is the latest. Due to the limited access to sectoral carbon emission data and the different sectoral classification in different input-output tables, the ISIC Rev 4.0 (UN, 2008) and the National Industries Classification (GB/T 4754–2017) from National Bureau of Statistics are used to ensure the consistent classification after sectoral consolidation process. The spherical distances between cities and the capital of their trade regions are taken from Google Maps. The rest of the world (ROW) is excluded because there are significant uncertainties in determining the distance between local (Beijing and Shanghai) and the ROW, which causes a significant result deviation in the gravity model and further leads to the result deviation. There are 65 regions involved in this study, and the IDs and names of these regions are presented in Table 1.

Table 1
The IDs and names of 65 regions.

Regional ID	Regional Name	Regional ID	Regional Name
R01	Local	R34	Spain
R02	Australia	R35	Sweden
R03	Austria	R36	Switzerland
R04	Belgium	R37	Turkey
R05	Canada	R38	United Kingdom
R06	Chile	R39	United States
R07	Colombia	R40	Argentina
R08	Costa Rica	R41	Brazil
R09	Czech Republic	R42	Brunei Darussalam
R10	Denmark	R43	Bulgaria
R11	Estonia	R44	Cambodia
R12	Finland	R45	Croatia
R13	France	R46	Cyprus
R14	Germany	R47	India
R15	Greece	R48	Indonesia
R16	Hungary	R49	Kazakhstan
R17	Iceland	R50	Lao People's Democratic Rep
R18	Ireland	R51	Malaysia
R19	Israel	R52	Malta
R20	Italy	R53	Morocco
R21	Japan	R54	Myanmar
R22	Korea	R55	Peru
R23	Latvia	R56	Philippines
R24	Lithuania	R57	Romania
R25	Luxembourg	R58	Russian Federation
R26	Mexico	R59	Saudi Arabia
R27	Netherlands	R60	Singapore
R28	New Zealand	R61	South Africa
R29	Norway	R62	Thailand
R30	Poland	R63	Tunisia
R31	Portugal	R64	Viet Nam
R32	Slovak Republic	R65	Mainland China
R33	Slovenia		

4. Results

4.1. The residential embodied carbon emission based on the CCG-MRIO model

The results of sectoral contributions on total embodied carbon emission at the 8-sector level are shown in Fig. 1. The sector aggregation has little impact on identifying the sector with the largest emission contribution between L1 and L2 datasets. Except for Beijing in 2012, which has different sectors with the largest emission, they are the “L1S3-Light Industry” (23.75 Mt) in L1 dataset and the “L1S8-Other Services” (23.05 Mt) in L2 dataset, and the “L1S3-Light Industry” has only 0.16 Mt less emission than “L1S8-Other Services” in L2 dataset, others all have the same sector with the largest emission. It is the “L1S5-Production and Supply of Electric Power, Heat Power, Gas, and Water” has the largest emission contribution in both L1 (41.09 Mt) and L2 (45.44 Mt) datasets in 2012 Shanghai, and the “L1S8-Other Services” has the largest emission contribution in both L1 and L2 dataset for Beijing (29.30 Mt in L1 dataset and 29.60 Mt in L2 dataset) and Shanghai (30.88 Mt in L1 dataset and 31.90 Mt in L2 dataset) in 2017.

Interestingly, the most apparent sector aggregation effect (SAE) on sectoral emission contributions does not necessarily occur in the aggregated sectors. The sector in 2012 of Beijing with the strongest SAE is “L1S6-Construction” (SAE is 43.74%), and this sector even has the strongest SAE in 2012 and 2017 for Shanghai (SAE in 2012 is 82.96%, SAE in 2017 is 25.84%). The construction sector is the same single sector under the three datasets, so its strong sector aggregation effect depicts that the emission contribution of a sector without sector aggregation process will also be affected by the aggregation process of other sectors. There is also no relationship between the sector aggregation effect and the number of aggregated sectors. For example, the “L1S4-Heavy Industry” contains 9 sectors and the “L1S7-Commerce and Transportation” includes 2 sectors in L2 dataset, the heavy industry has a stronger sector aggregation effect than that in commerce and transportation in 2012 Beijing, but it turns to the opposite results in 2017. Such irrelevant property also occurs at the 22-sector level, as presented in Fig. 2, which shows the sectoral emission contributions of L2 and L3 datasets at the 22-sector level.

The sectoral emission results in 2012 have more evident discrepancy than that in 2017 of Beijing and Shanghai at 22-sector level. The SAE ranges from −0.35% to 16.89% in 2017 of Beijing (it ranges from −44.05% to 170.57% in 2012), and ranges from −9.60% to 3.06% in 2017 of Shanghai (it ranges from −45.53% to 66.48% in 2012), the range fluctuations are small in 2017. The strongest SAE on sectoral emission contribution in 2012 is the “L2S18-Production and Distribution of Water” in Beijing (SAE is 170.57%) and the “L2S19-Construction” in Shanghai (SAE is 66.48%). The sectoral emission contribution of “L2S17-Production and Supply of Electric Power, Heat Power and Gas” is also noteworthy despite its relative less obvious SAE than the above two sectors (SAEs are −28.45% and −30.66% in Beijing and Shanghai, respectively), its absolute contribution has decreased by 4.33 Mt from L2 to L3 dataset in Beijing, and decreased by 13.67 Mt from L2 to L3 dataset in Shanghai. The strong SAEs of these three sectors derive from the input-output structure differences between L2 and L3 datasets, as their carbon intensities and final products for residential consumptions are consistent in L2 and L3 datasets. In contrast, the aggregated sector in L2 dataset, such as “L2S22-Other Services” (it contains 9 sub-sectors in L3

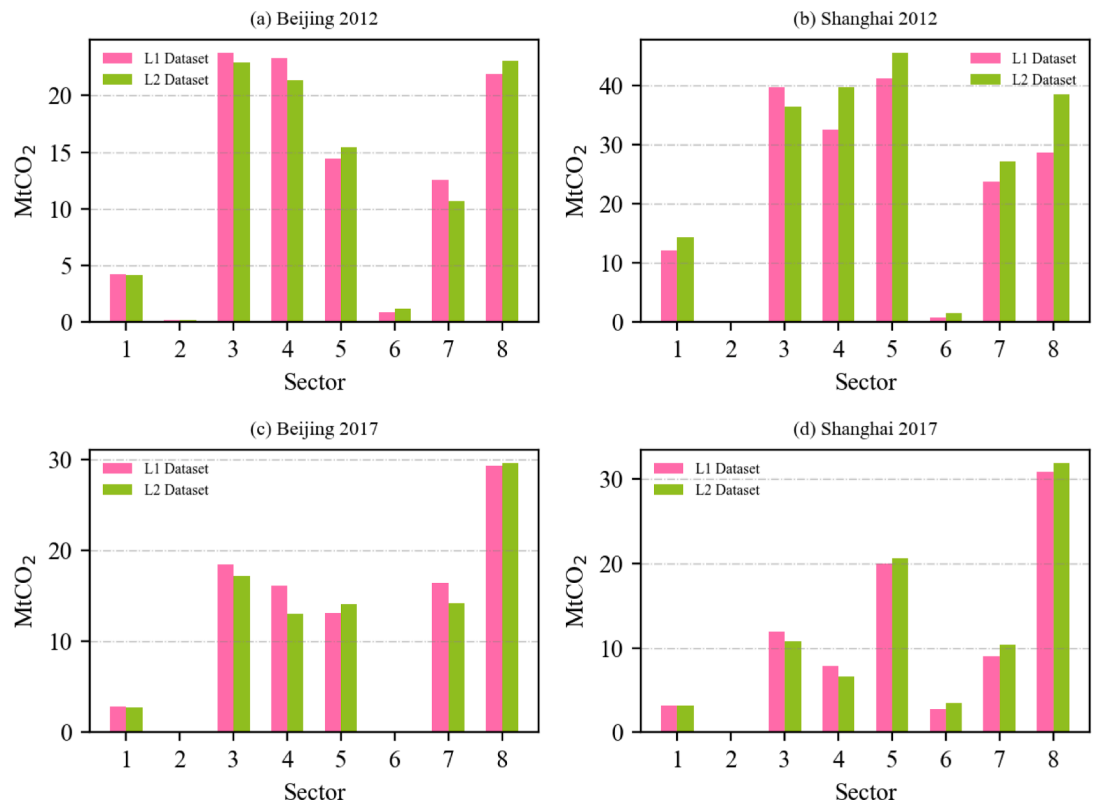

Fig. 1. Sectoral contributions on residential embodied carbon emissions of Beijing and Shanghai at 8-sector level.

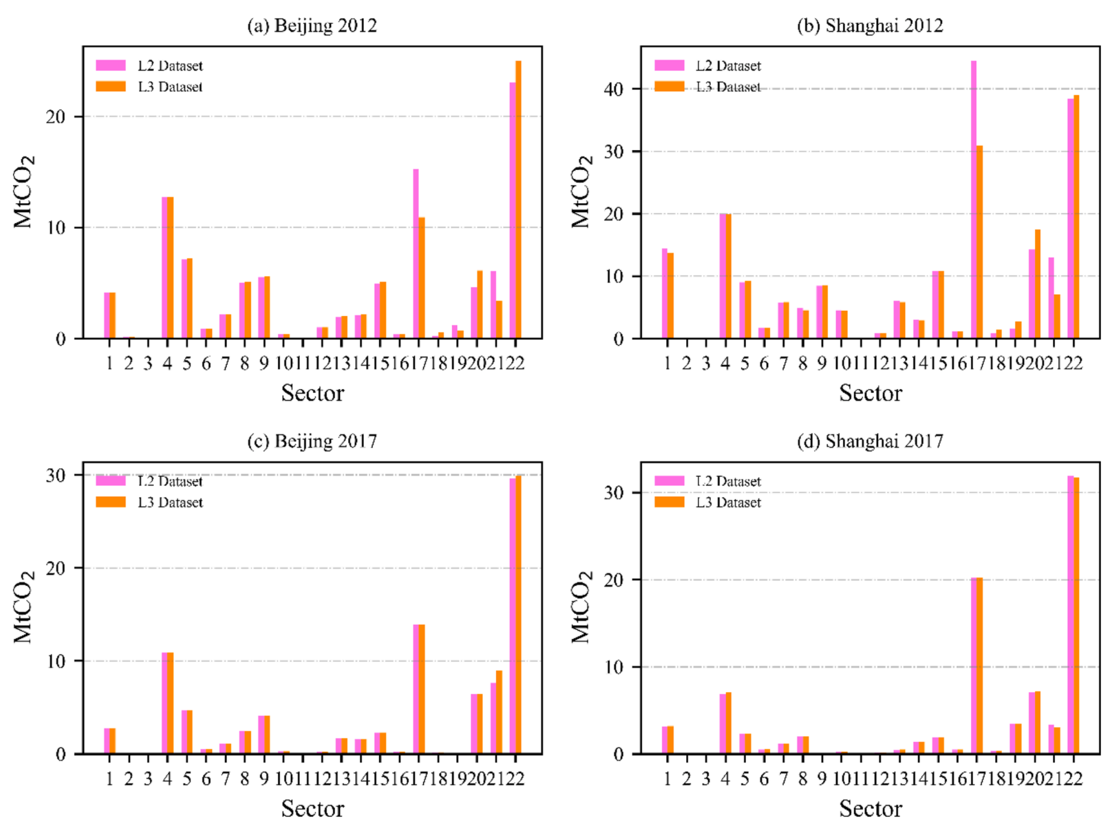

Fig. 2. Sectoral contributions on residential embodied carbon emissions of Beijing and Shanghai in L2 and L3 datasets at 22-sector level.

dataset), its SAEs are only 8.60% and 1.59% in Beijing and Shanghai in 2017 respectively. Therefore, the input-output structure change from the merger operation of one sector could affect the emission contribution of other sectors, and may lead to wrong judgment if researchers only focus on identifying the sector with the largest contribution.

The sector aggregation also leads to the regional emission contribution differences among the three datasets. Since the emission contribution of each region is the integration of its sectoral emission contributions, the regional contribution is more vulnerable to the impact of sectoral aggregation than the sectoral contribution, and the contribution fluctuates is more complex at different sectoral levels, as presented in Fig. 3. The average SAE values of Beijing are −5.46% and −2.41% in 2012 and 2017 in L1 dataset, and the values are 32.68% and 74.09% in 2012 and 2017 in L3 dataset; the average SAE values of Shanghai are −7.06% and −7.67% in 2012 and 2017 in L1 dataset, and the values are 11.28% and 7.86% in 2012 and 2017 in L3 dataset, indicate that the regional emission contributions tends to decrease in L1 dataset after sector consolidation in L2 dataset, while the regional emission contributions tend to increase in L3 dataset after sector expansion in L3 dataset. The average absolute SAE values of L1 and L3 datasets reflect that the regional emission contributions in L3 dataset were affected by relatively stronger SAE than that in L1 dataset, as the average absolute SAE values of L1 dataset are 10.70% and 11.59% in 2012 and 2017 in Beijing, while the values of L3 dataset are 38.84% and 80.54% in 2012 and 2017 in Beijing; the average absolute SAE values of L1 dataset are 18.59% and 17.41% in 2012 and 2017 in Shanghai, while the values of L3 dataset are 28.09% and 17.18% in 2012 and 2017 in Shanghai. In addition, the L3 dataset tends to have more extreme SAE values than L1 dataset, as the strongest SAE on regional emission contributions in these two cities all appeared on L3 dataset in 2012 and 2017 (the SAE of R50-Lao People's Democratic Rep is 417.77% in Fig. 3(a), the SAE of R17-Iceland is 159.17% in Fig. 3(b), the SAE of R17-Iceland is 972.00% in Fig. 3(c), the SAE of R22-Korea is 151.40% in Fig. 3(d)). These differences of SAEs in L1 and L3 datasets prove that the regional emission contributions in L3 dataset tend to have more intensive fluctuations than that in L1 dataset, resulting from the unreal carbon intensities of expansion sectors in L3 dataset.

It is worth noting that the extreme SAE values tend to appear on the regions with little emission contributions in L2 dataset, as the contribution of R50-Lao People's Democratic Rep on Beijing's residential embodied emission in 2012 is only 0.028 Mt, the contribution of R17-Iceland on Beijing's residential embodied emission in 2017 is only 0.003 Mt, the contribution of R17-Iceland on Shanghai's residential embodied emission in 2012 is only 0.010 Mt (the contribution of R22-Korea on Shanghai's residential embodied emission in 2017 is 1.013

Table 2
Top 5 regions with the largest emission contributions on residential embodied emission of Beijing and Shanghai in three datasets.

	L1 dataset	L2 dataset	L3 dataset
Beijing 2012	R1, R65, R39, R22, R14	R1, R65, R39, R14, R22	R1, R65, R39, R14, R22
Shanghai 2012	R1, R65, R39, R47, R64	R1, R65, R39, R47, R64	R1, R65, R39, R47, R21
Beijing 2017	R65, R1, R39, R14, R47	R1, R65, R39, R14, R47	R1, R65, R39, R14, R47
Shanghai 2017	R1, R65, R39, R47, R64	R1, R65, R39, R47, R21	R1, R65, R39, R22, R21

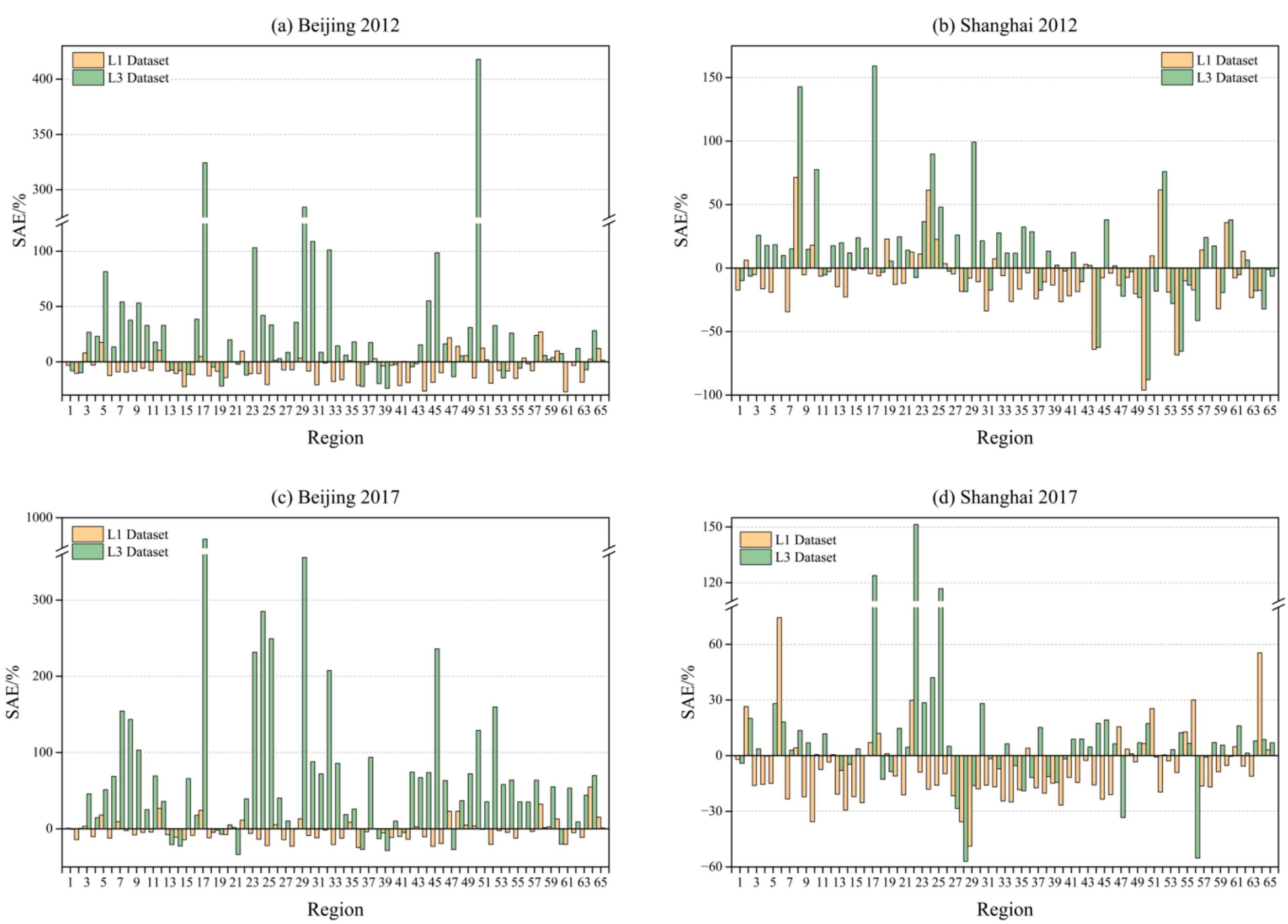

Fig. 3. Sector aggregation effect on regional emission contributions of Beijing and Shanghai in L1 and L3 datasets at 22-sector level of L2 dataset.

Mt). Therefore, when the intensity assumption is used to expand the sector to obtain more sectoral information, it may also lead to a large deviation in the regional emission contributions, especially for regions with small contributions, but it will not lead to a deviation in the identification of key emission contribution regions, as shown in Table 2.

4.2. Sector aggregation effect on structural path analysis results

The top 30 transmission paths under three datasets in 2012 and 2017 of Beijing and Shanghai are identified based on the 8-sector level of the L1 dataset and the 22-sector level of the L2 dataset, the path results are presented in **Appendix C**. Due to the large emission contributions of Local (R01) and Mainland China (R65), most of the critical embodied carbon emission transmission paths also originate from these two regions. The paths with the largest embodied carbon emission are consistent between L1 and L2 datasets at the 8-sector level, it is the same path 'R65.L1S4→R65.L1S4→R65.L1S4' in 2012 (5.512 Mt in L1 dataset and 3.501 Mt in L2 dataset) and 2017 (5.984 Mt in L1 dataset and 3.468 Mt in L2 dataset) for Beijing, and the same path 'R01.L1S5→R01.L1S5→R01.L1S5' in 2012 (16.984 Mt in L1 dataset and 12.864 Mt in L2 dataset) and 2017 (7.769 Mt in L1 dataset and 7.424 Mt in L2 dataset) for Shanghai, while there are different paths with the largest embodied emission between L2 and L3 datasets at the 22-sector level.

The sector aggregation has a relative weaker effect on path results between L1 and L2 datasets than that between L2 and L3 datasets, not only for L1 dataset has the same emission path with the largest embodied emission as L2 dataset, but for L1 dataset has more identical paths with L2 dataset than L3 dataset. In the listed 30 paths at 8-sector level, the L1 and L2 datasets have 21, 26, 21, 21 same paths in 2012 and 2017 for Beijing and Shanghai. However, the L2 and L3 datasets have only 8, 5, 15, 16 same paths in the listed 30 paths at 22-sector level in 2012 and 2017 for Beijing and Shanghai, which shows that expanding sectors by adopting the intensity assumption will lead to significant path differences.

There are two cases of path differences, the first is that part of the same path is missing, which can be supplemented by further adjusting the path threshold. For example, the largest emission path in L2 dataset is the 'R65.L2S17→R65.L2S17→R65.L2S17' for Beijing in 2012 (3.247 Mt) and 2017 (3.050 Mt), while the largest emission path in L3 dataset is the 'R65.L2S17' for Beijing in 2012 (2.580 Mt) and 2017 (2.273 Mt) at the 22-sector level, the two datasets both have recognized that the sector 'R65.L2S17' contains large embodied emissions, the difference is that the L2 dataset identifies the high emission characteristics of the sector as both the final consumption sector and the upstream supply sector, while the L3 dataset only identifies the high emission characteristics of the sector in its final consumption. The largest emission path in Shanghai has the same situation, it is the 'R01.L2S17→R01.L2S17→R01.L2S17' in L2 dataset in 2012 (12.801 Mt) and 2017 (7.347 Mt), while the path is 'R01.L2S17' in L3 dataset in 2012 (8.096 Mt) and 2017 (5.888 Mt) at the 22-sector level. When researchers realize that the identified path is missing, they can re-identify the path by reducing the threshold to complete the missing part of the path. The other case in path differences is the path supplement from some other regions, which is mainly reflected in the path recognition results in L3 dataset, the supplemented paths are shown in Table 3. The regions of the listed paths in Table 3 only appear in the listed top 30 paths in L3 dataset, such as path 'R60.L2S20' in 2012 for Beijing, which indicates the transport, storage, and post sector of R60-Singapore has a large contribution (0.241 Mt) to the residential consumption emission in Beijing, while the L2 dataset failed to identify this path. These additional regional key transmission paths provided by L3 dataset are undoubtedly valuable for seeking emission reduction methods from trade activities, especially when L3 datasets ensures that other critical paths (such as the path with largest embodied emission) are consistent with that in L2 dataset by threshold adjustment.

Table 3
The supplemented paths in L3 dataset at 22-sector level.

Beijing 2012	Beijing 2017	Shanghai 2012	Shanghai 2017
R60. L2S20	R49. L2S17	R60. L2S20	R42. L2S17
R49. L2S17	R60. L2S20		R22. L2S17→R22. L2S22
R59. L2S17	R61. L2S17		R59. S17
	R42. L2S17		R54. S17

4.3. Sector aggregation effect on structural decomposition analysis results

The sector aggregation effects on the sectoral emission contributions of three factors at 8-sector level are shown in Fig. 4. The contributions of input-output structure factor (*ps*) and final demand factor (*fd*) have more obvious sector aggregation effects than carbon intensity factor (*ci*), for the average absolute values of sector aggregation effect of carbon intensity factor, input-output structure factor, and final demand factor are 3.34%, 4.42% and 7.77% for Beijing, and the values are 6.09%, 20.63% and 22.47% for Shanghai. The "L1S6-Construction" has both the strongest sector aggregation effects of input-output structure factor and final demand factor for Beijing (−8.20% for *ps* and −32.53% for *fd*) and Shanghai (−85.09% for *ps* and 125.09% for *fd*), since the "L1S1-Agriculture" has weak sector aggregation effects on its factor contributions and this sector also has no sub-sectors, so the sector aggregation effect on sectoral factor contribution has no relationship with the number of sub-sectors. The sector aggregation even leads to directional changes in input-output structure effect while the sectoral contribution of other two factors has no direction changes, which will lead to cognitive bias on the nature of factor contributions. For example, the input-output structure factor of "L1S7-Commerce and Transportation" in Beijing prompts 0.40 Mt emission reduction in L1 dataset, but it turns to contribute 0.25 Mt emission growth in L2 dataset, making it hard to determine the role of the input-output structure on the emission changes of the sector. Therefore, the utility change of input-output structural factors after sector merger should be treated with caution.

The sector aggregation effects on factor contribution results at 22-sector level are presented in Fig. 5. The strongest sector aggregation effect concentrated in a few sectors as "L2S18-Production and Distribution of Water", "L2S19-Construction", "L2S20-Transport, Storage, and Post", and "L2S21-Wholesale, Retail Trades, Hotels and Catering". Even though the emission intensity and residential consumption input of some sectors are the same in the two datasets, the differences of input-output structure between L2 and L3 datasets will also lead to changes in carbon intensity effect and final demand effect, not to mention the input-output structure effect itself. For example, the "L2S18-Production and Distribution of Water" has the same residential consumption input between L2 and L3 datasets, but the sector aggregation effect on its final demand factor contribution is −189.68% for Beijing and −78.88% for Shanghai. The "L2S19-Construction" has the same carbon intensity between L2 and L3 datasets, but the sector aggregation effect on its carbon intensity factor contribution is −11.89% for Beijing and −280.66% for Shanghai. The sector aggregation also leads to directional changes in factor impacts of some sectors (for example, the carbon intensity effect of "L2S20-Transport, Storage, and Post" changed from negative in L2 dataset to positive in L3 dataset for both Beijing and Shanghai, the input-output effect of "L2S18-Production and Distribution of Water" has the same direction changes, the final demand effect of "L2S21-Wholesale, Retail Trades, Hotels and Catering" changed from negative in L2 dataset to positive in L3 dataset for Shanghai).

The sector aggregation also impacts on regional factor emission contributions, and the results are shown in Fig. 6. There are no obvious differences between the sector aggregation effect intensities of L1 and L3 datasets in carbon intensity factor and input-output structure factor as a whole, while the L1 dataset tends to has more extreme sector aggregation values, such as these two factor contributions of R52-Malta on the residential embodied emission changes of Beijing (BSA_{ci} is 304.50% and BSA_{ps} is −293.32%) and of Shanghai (BSA_{ci} is 313.98% and BSA_{ps} is

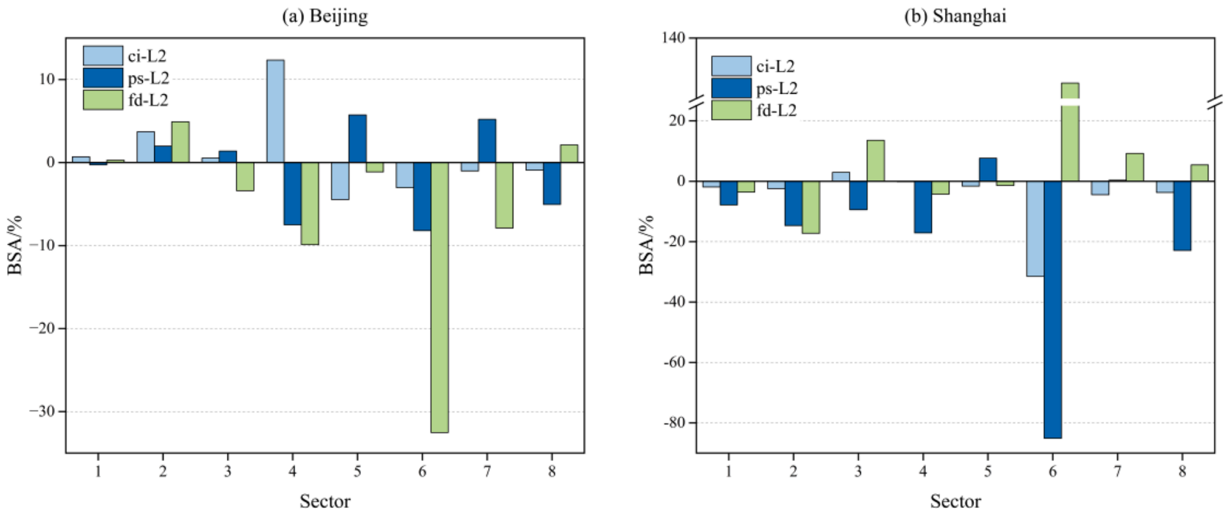

Fig. 4. Sector aggregation effects on sectoral SDA results in (a) Beijing and (b) Shanghai at 8-sector level, 2012–2017.

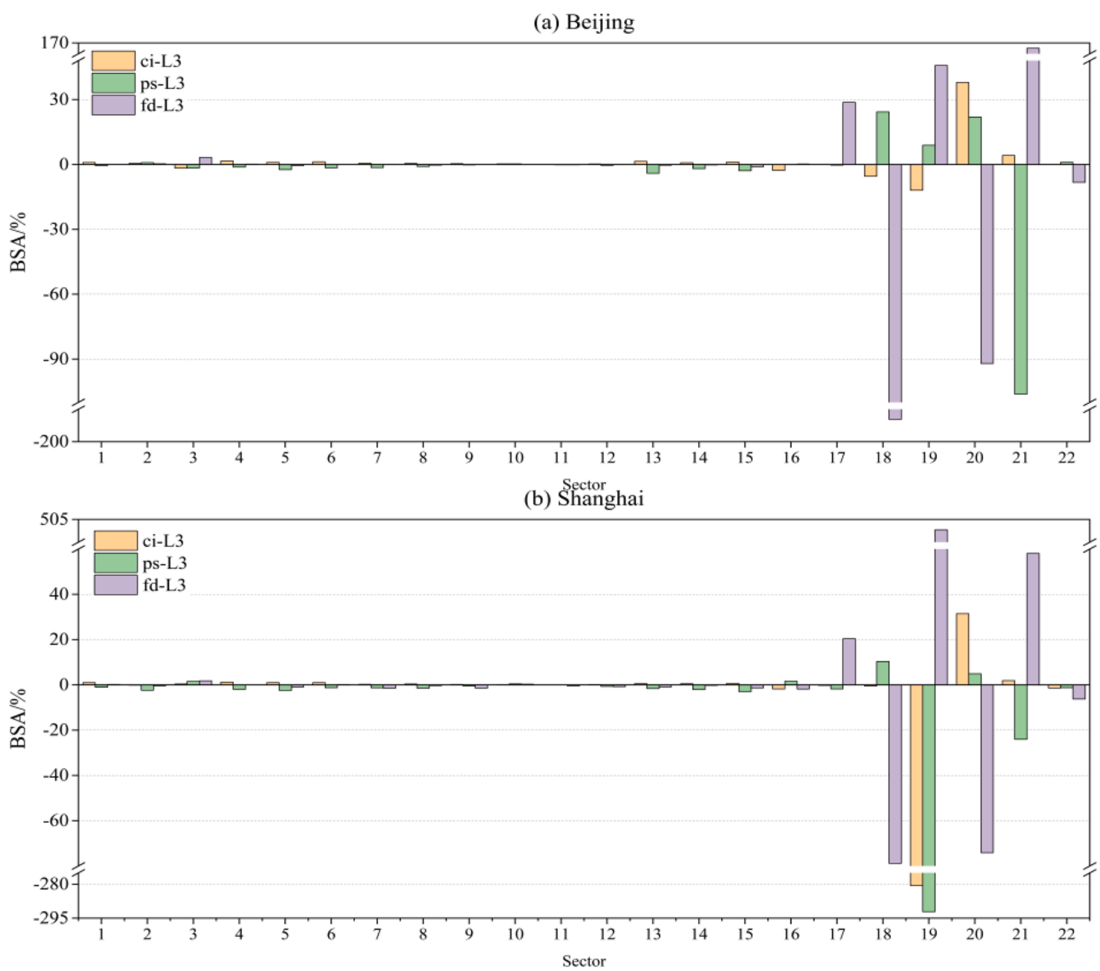

Fig. 5. Sector aggregation effects on SDA of sectoral emission contributions in (a) Beijing and (b) Shanghai at 22-sector level, 2012–2017.

−298.27%), which indicate that the carbon intensity factor in L1 dataset is more inclined to play a role in promoting the increase of R52-Malta contribution on the residential embodied emissions in Beijing and Shanghai than that in L2 dataset, and the input-output factor in L1 dataset is more inclined to play a role in inhibiting the increase of R52-Malta contribution on the residential embodied emission in Beijing and Shanghai than that in L2 dataset. For the final demand factor, the sector aggregate effect in L3 dataset is more significant than that in L1 dataset, it tends to promoting more increase of regional contributions on the residential embodied emissions in Beijing in L3 dataset than that in L2 dataset, such as R50-Lao People's Democratic Rep (BSA_{fd} is 478.48%), while the case is opposite in Shanghai, such as R29-Norway (BSA_{fd} is −117.74%). Therefore, the sectoral aggregation will lead to deviations between the factor contributions of L1 and L3 datasets (whether in

Fig. 6. Sector aggregation effects on SDA of regional emission contributions in (a) Beijing and (b) Shanghai at 22-sector level, 2012–2017.

sectoral or regional factor contributions) and L2 datasets, and even lead to directional changes in some factor contributions, which reminds us to carefully consider the changes in factor contributions when further integrating or expanding sectors.

5. Discussion

The city-centric global multi-region input-output (CCG-MRIO) model provides a bridge linking the carbon emission research between the internal consumption of a single city and its international trade activities, and different levels of sectoral aggregation may produce different carbon emission results due to the complex model-building process. Compared with L3 dataset, the results in L1 dataset have weaker sector aggregation effects and less deviation from L2 database, that is because the data in L1 database is further processed from L2 dataset, and all of them are real data. So if the purpose of one study is to find some highly aggregated sectors with significant emission and their critical emission paths, the results of L1 dataset can simplify the calculation and ensure the results' accuracy. However, L1 and L3 datasets do not perform well in factor decomposition results due to some directional deviations, especially in the contribution positioning of the input-output structure factor. Therefore, the contribution of the input-output structure factor needs to be discussed according to the sector aggregation level. The optimal choice is to use the highest sectoral resolution to preserve the largest sectoral detail, as suggested by de Koning et al. (2015) and Zhang et al. (2019).

The L3 dataset by adopting the consistent intensity assumption has caused some emission discrepancy, but this does not mean that it is useless to expand sectors by adopting assumptions. On the contrary, the decomposition of highly aggregated sectors can more accurately grasp the key emission sectors, so as to facilitate carbon emission reduction according to the different sectoral emission characteristics. If the sector matching of the carbon emission database is ignored and only considers how to maximize the use of the real data of sector emissions, more real emission results can be obtained. For example, the sub-sector carbon emission data of other regions are provided from OECD database except for R01-Local and R65-Mainland China, so the consistent intensity assumption can be only applied to the carbon emission intensities for sub-sectors in R01-Local and R65-Mainland China while the carbon emission intensities of sub-sectors in other regions are obtained by using the real data. The carbon emission calculated with this method have little differences from those obtained with the consistent intensity assumption, for the average deviations in sectoral emissions are only 0.49% in 2012 and 0.27% in 2017 for Beijing, and they are only 0.98% in 2012 and 0.66% in 2017 for Shanghai. For the average deviation in regional emissions, they are only 1.78% in 2012 and 1.45% in 2017 for Beijing, and they are 0.78% in 2012 and 1.02% in 2017 for Shanghai. The factor contribution results also have little deviation, for the deviations in sectoral and regional factor contribution results all less than 10% for Beijing and Shanghai, except for the average deviation in regional carbon intensity factor contribution is 23.17%, which mainly from the carbon intensity factor of R51-Malaysia, it has prompted more 0.02 emission growth than that in the result by using the consistent intensity assumption. Still, because the contribution direction has not changed and the growth is small, the results also not be affected. The path results by using the real data in OECD are presented in **Appendix D**, the paths with the largest emission are consistent with that in L3 dataset, the paths listed are only different in sequence, and basically cover all the critical path information of the L3 database. Therefore, L3 database with the sectoral consistent intensity assumption can basically reflect the real emission, factor contribution and key path information.

There are still some limitations in this study that need to be addressed in future research. Except for the sectoral expansion by adopting consistent intensity assumption, there are still other methods to expand sectors to get the missing sectoral carbon intensity data, selecting suitable method which is closer to the actual sectoral emission situation will better reduce the impact of the sector aggregation effect. In addition, a more detailed sector level is not included in this study due to the sector fineness limit of the input-output tables, considering some input-output tables containing more sectors and adopt more accurate trade matrix estimation method can be analyzed in the future.

6. Conclusion

Based on the city-centric global multi-region input-output (CCG-MRIO) model, this paper has studied the sector aggregation effect on the residential embodied carbon emission of Beijing and Shanghai. From the view of simplifying the data calculation, the 8-sector level can obtain the almost same sectoral and regional embodied emission contribution results, as well as the path results, so it is appropriate to only locate some high aggregate sectors, key regions, or key emission paths with high embodied emissions. Although expanding the sector in an assumed way will lead to deviations in sectoral and regional emission results, the positioning of key sectors and regions is basically accurate, so it is also appropriate to use the intensity assumption to decompose some highly aggregated sectors in consideration of the need to obtain more information on sectoral emission contributions. However, there are directional changes in factor contributions at the sector level with higher aggregation or sectoral expansion, especially in the input-output structure factor. Therefore, the most detailed sectoral with real data is preferred in factor analysis to ensure accuracy. Adopting a consistent intensity assumption to expand sectors is prefered in path analysis for it ensure the accuracy of critical paths and provides some extra path information.

The results of this study provide a reference for the sector aggregation level selected in similar studies in the future. The result has the same reference value for other final consumptions that only the calculation matrix is replaced. The changes in input-output structure, regional emission contributions, and some path omission should be paid attention at different sectoral levels. It is suggested that the appropriate assumption and the level of sector aggregation should be selected on the basis of meeting specific research needs. The consistent assumptions studied in this paper provide guidance for obtaining more detailed characteristics of sectoral emissions with simple data process works, especially for high-aggregated industries such as service industries, whose sub-sector emission data are usually challenging to obtain.

CRediT authorship contribution statement

GY Liu, D Xu and H Li contributed to methodology development, conducted validation, and contributed to the writing of early drafts and final draft review and editing; GY Liu and H Li were responsible for overall project supervision, conceptualization, project management; FX Meng, NY Yan, F Agostinho, CMVB Almeida and BF Giannetti contributed to the data analysis and revision checking.

Declaration of Competing Interest

The authors declare that they have no known competing financial interests or personal relationships that could have appeared to influence the work reported in this paper.

Data availability

Data will be made available on request.

Acknowledgements

This work is supported by the Fund for the National Natural Science Foundation of China (No. 52070021), Key Special Project for Introduced Talents Team of Southern Marine Science and Engineering Guangdong

Laboratory (Guangzhou) (GML2019ZD0403) and the 111 Project (No. B17005).

Supplementary materials

Supplementary material associated with this article can be found, in the online version, at doi:10.1016/j.ecolmodel.2023.110487.

References

Bouwmeester, M.C., Oosterhaven, J., 2013. Specification and aggregation errors in environmentally extended input-output models. Environ. Resour. Econ. (Dordr) 56 (3), 307–335. https://doi.org/10.1007/s10640-013-9649-8.

Cansino, J.M., Roman, R., Ordonez, M., 2016. Main drivers of changes in CO2 emissions in the Spanish economy: a structural decomposition analysis. Energy Policy 89, 150–159. https://doi.org/10.1016/j.enpol.2015.11.020.

CEADs. (2022). Multi-regional input and output of Chinese cities, https://www.ceads.net.cn/.

Dawkins, E., Moran, D., Palm, V., et al., 2019. The Swedish footprint: a multi-model comparison. J. Clean. Prod. 209, 1578–1592. https://doi.org/10.1016/j.jclepro.2018.11.023.

de Koning, A., Bruckner, M., Lutter, S., et al., 2015. Effect of aggregation and disaggregation on embodied material use of products in input-output analysis. Ecol. Econ. 116, 289–299. https://doi.org/10.1016/j.ecolecon.2015.05.008.

Dietzenbacher, E., Los, B., 1998. Structural decomposition techniques: sense and sensitivity. Econ. Syst. Res. 10 (4), 307–323.

Fang, D., Yang, J., 2021. Drivers and critical supply chain paths of black carbon emission: a structural path decomposition. J. Environ. Manag. 278 https://doi.org/10.1016/j.jenvman.2020.111514.

Hoekstra, R., van der Bergh, J., 2003. Comparing structural and index decomposition analysis. Energy Econ. 25 (1), 39–64. https://doi.org/10.1016/s0140-9883(02)00059-2.

Hong, J.K., Shen, Q.P., Xue, F., 2016. A multi-regional structural path analysis of the energy supply chain in China's construction industry. Energy Policy 92, 56–68. https://doi.org/10.1016/j.enpol.2016.01.017.

Jiang, M.H., An, H.Z., Gao, X.Y., et al., 2021. Structural decomposition analysis of global carbon emissions: the contributions of domestic and international input changes. J. Environ. Manag. 294 https://doi.org/10.1016/j.jenvman.2021.112942.

Lenzen, M., 2011. Aggregation versus disaggregation in input-output analysis of the environment. Econ. Syst. Res. 23 (1), 73–89. https://doi.org/10.1080/09535314.2010.548793.

Lin, J., Hu, Y., Zhao, X., et al., 2017. Developing a city-centric global multiregional input-output model (CCG-MRIO) to evaluate urban carbon footprints. Energy Policy 108, 460–466. https://doi.org/10.1016/j.enpol.2017.06.008.

Liu, H.G., Liu, W.D., Fan, X.M., et al., 2015. Carbon emissions embodied in demand-supply chains in China. Energy Econ. 50, 294–305. https://doi.org/10.1016/j.eneco.2015.06.006.

Liu, X.Y., Zhang, L.X., Hao, Y., et al., 2022. Increasing disparities in the embedded carbon emissions of provincial urban households in China. J. Environ. Manag. 302 https://doi.org/10.1016/j.jenvman.2021.113974.

Ma, R.F., Zheng, X.Q., Zhang, C.X., et al., 2022. Distribution of CO2 emissions in China's supply chains: a sub-national MRIO analysis. J. Clean. Prod. 345 https://doi.org/10.1016/j.jclepro.2022.130986.

OECD, 2021. OECD Inter-Country Input-Output Database. http://oe.cd/icio.

Shan, Y., Guan, D., Zheng, H., et al., 2018. Data Descriptor: china CO2 emission accounts 1997-2015. Sci. Data 5. https://doi.org/10.1038/sdata.2017.201.

Shan, Y., Huang, Q., Guan, D., et al., 2020. China CO2 emission accounts 2016-2017. Sci. Data 7 (1). https://doi.org/10.1038/s41597-020-0393-y.

Shi, J.L., Li, H.J., An, H.Z., et al., 2020. What induces the energy-water Nexus in China's supply chains? Environ. Sci. Technol. 54 (1), 372–379. https://doi.org/10.1021/acs.est.9b04277.

Steen-Olsen, K., Owen, A., Hertwich, E.G., et al., 2014. Effects of sector aggregation on CO2 multipliers in multiregional input-output analyses. Econ. Syst. Res., 26 (3), 284–302. https://doi.org/10.1080/09535314.2014.934325.

Su, B., Ang, B.W., 2012a. Structural decomposition analysis applied to energy and emissions: some methodological developments. Energy Econ. 34 (1), 177–188. https://doi.org/10.1016/j.eneco.2011.10.009.

Su, B., Ang, B.W., 2012b. Structural decomposition analysis applied to energy and emissions: aggregation issues. Econ. Syst. Res. 24 (3), 299–317. https://doi.org/10.1080/09535314.2012.677997.

Su, B., Ang, B.W., 2017. Multiplicative structural decomposition analysis of aggregate embodied energy and emission intensities. Energy Econ. 65, 137–147. https://doi.org/10.1016/j.eneco.2017.05.002.

Su, B., Ang, B.W., Li, Y.Z., 2019. Structural path and decomposition analysis of aggregate embodied energy and emission intensities. Energy Econ. 83, 345–360. https://doi.org/10.1016/j.eneco.2019.07.020.

Su, B., Ang, B.W., Liu, Y., 2021. Multi-region input-output analysis of embodied emissions and intensities: spatial aggregation by linking regional and global datasets. J. Clean. Prod. 313 https://doi.org/10.1016/j.jclepro.2021.127894.

Su, B., Huang, H.C., Ang, B.W., et al., 2010. Input-output analysis of CO2 emissions embodied in trade: the effects of sector aggregation. Energy Econ. 32 (1), 166–175. https://doi.org/10.1016/j.eneco.2009.07.010.

UN, 2008. International standard industrial classification of all economic activities (ISIC), revision 4. Statistical Papers, Series M (4), Rev 4. United Nations, New York.

Wang, C., Zhan, J.Y., Li, Z.H., et al., 2019a. Structural decomposition analysis of carbon emissions from residential consumption in the Beijing-Tianjin-Hebei region, China. J. Clean. Prod. 208, 1357–1364. https://doi.org/10.1016/j.jclepro.2018.09.257.

Wang, H., Ang, B.W., Su, B., 2017. Assessing drivers of economy-wide energy use and emissions: IDA versus SDA. Energy Policy 107, 585–599. https://doi.org/10.1016/j.enpol.2017.05.034.

Wang, J., Du, T., Wang, H., et al., 2019b. Identifying critical sectors and supply chain paths for the consumption of domestic resource extraction in China. J. Clean. Prod. 208, 1577–1586. https://doi.org/10.1016/j.jclepro.2018.10.151.

Wang, M., Feng, C., 2021. The inequality of China's regional residential CO2 emissions. Sustain. Prod. Consumption 27, 2047–2057. https://doi.org/10.1016/j.spc.2021.05.003.

Wang, Q., Yang, X., 2020. Imbalance of carbon embodied in South-South trade: evidence from China-India trade. Sci. Total Environ. 707 https://doi.org/10.1016/j.scitotenv.2019.134473.

Wang, S.G., Chen, B., 2021. Unraveling energy-water nexus paths in urban agglomeration: a case study of Beijing-Tianjin-Hebei. Appl. Energy 304. https://doi.org/10.1016/j.apenergy.2021.117924.

Wang, Y., Li, X.M., Sun, Y., et al., 2020. Linkage analysis of economic consumption, pollutant emissions and concentrations based on a city-level multi-regional input output (MRIO) model and atmospheric transport. J. Environ. Manag.. 270 https://doi.org/10.1016/j.jenvman.2020.110819.

Wood, R., Lenzen, M., 2003. An application of a modified ecological footprint method and structural path analysis in a comparative institutional study. Local Environ. 8 (4), 365–386. https://doi.org/10.1080/13549830306670.

Xie, R., Huang, L.Y., Tian, B.S., et al., 2019. Differences in changes in carbon dioxide emissions among china's transportation subsectors: a structural decomposition analysis. Emerg. Mark. Financ. Trade 55 (6), 1294–1311. https://doi.org/10.1080/1540496x.2018.1526076.

Yan, Y.F., Wang, R., Zheng, X.X., et al., 2020. Carbon endowment and trade-embodied carbon emissions in global value chains: evidence from China. Appl. Energy 277. https://doi.org/10.1016/j.apenergy.2020.115592.

Yang, L.G., Li, L.L., Zhu, K.F., et al., 2020. Structural path analysis of China's coal consumption using input-output frameworks. Environ. Sci. Pollut. Res. 27 (7), 6796–6812. https://doi.org/10.1007/s11356-019-07176-6.

Zhang, D., Caron, J., Winchester, N., 2019. Sectoral aggregation error in the accounting of energy and emissions embodied in trade and consumption. J. Ind. Ecol. 23 (2), 402–411. https://doi.org/10.1111/jiec.12734.

Zhang, J.H., Wang, H.M., Ma, L., et al., 2021. Structural path decomposition analysis of resource utilization in China, 1997-2017. J. Clean. Prod. 322 https://doi.org/10.1016/j.jclepro.2021.129006.

Zhao, Y.H., Cao, Y., Shi, X.P., et al., 2021. Critical transmission paths and nodes of carbon emissions in electricity supply chain. Sci. Total Environ. 755 https://doi.org/10.1016/j.scitotenv.2020.142530.

Zhou, D.Q., Zhou, X.Y., Xu, Q., et al., 2018. Regional embodied carbon emissions and their transfer characteristics in China. Structural Change and Econ. Dynam. 46, 180–193. https://doi.org/10.1016/j.strueco.2018.05.008.